

25 creating the models) and testing (for validating the developed models) data based on a statistical
26 process. The procedure for preparing the data and developing and validating the models is presented
27 in detail in this paper. The main advantage of the proposed models over a conventional and neural
28 network and most GP (Genetic Programming)-based constitutive models is that they provide the
29 optimum structure for the material constitutive model representation as well as its parameters,
30 directly from raw experimental (or field) data. EPR can learn nonlinear and complex material
31 behavior without any prior assumptions on the constitutive relationships. The proposed algorithm
32 captures and transparently presents relationships between contributing parameters in polynomial
33 expressions providing the user with a clear insight into the problem. EPR-based model predictions
34 demonstrated an excellent agreement with the unseen simulated data used for validating the
35 developed model. A parametric study on the presented models was conducted to investigate the
36 effects of the contributing parameters on model predictions and the consistency of the parameter
37 relationships with the database. Results of the parametric study showed that the effects of variations
38 in the contributing parameters on EPR predictions are in line with the expected behavior. The merits
39 and advantages of the proposed technique are discussed in the paper.

40

41 **Keywords:** Sheet piles/Cut-off walls; Seepage flow rate, Evolutionary computation; Data mining

42 **1. Introduction**

43 Desirable safety of the water-retaining structures is identified as the top priority of geotechnical
44 research attention which is foundational to broader research in the field. The discharge flow rate at
45 the downstream side of a water retaining structure, as a seepage output quantity, remains the central
46 part of the safe design of the structure. The high values of the discharge flow rate can endanger the
47 water retaining structure stability. Use should be made of installed vital systems called sheet piles
48 for reducing the values of downstream discharge flow rate at a flow region or under the foundation

49 of a dam. The seepage beneath the sheet pile follows a specific differential equation in calculating
50 discharge flow rate – similar to most seepage-related problems in geotechnical engineering. Beyond
51 that, researchers for solving the seepage governing equation and computing the flow rate discharge
52 have employed various methods. The analytical and numerical methods have been performed more
53 broadly.

54 A variational iteration method with fractional derivatives as an analytical method to solve the
55 nonlinear seepage flow into porous media was suggested by He [1]. Handling a finite difference
56 method based on boundary-fitted coordinate transformation to analyze the steady-state seepage
57 with a free surface in the isotropic and homogeneous embanked dam was carried out by Jie et al. [2].
58 In analyzing the two and three-dimensional seepage problems using finite difference methods, so-
59 called boundary polynomial interpolation was adopted by Fukuchi [3]. Relying on two practical
60 approaches suggested in the literature, Bresciani et al. [4] applied a finite volume-based method to
61 find out the solutions of groundwater flow through earth dams. Their proposed methods merged the
62 most beneficial advantages of adaptive and fixed mesh techniques. A coupled finite element-based
63 method to model the transient seepage flow beneath a concrete dam has been employed by Ouria et
64 al. [5]. Kazemzadeh-Parsi and Daneshmand [6] have exerted a smoothed fixed grid finite element
65 method to analyze three-dimensional unconfined seepage of complex geometries, heterogeneous,
66 and anisotropic porous media. Rafiezadeh and Ataie-Ashtiani [7] developed a coded computer
67 program based on the boundary element method to analyze three-dimensional confined seepage
68 problems under dams. The unconfined seepage problems by the natural element method have been
69 simulated by Jie et al. [8]. Mesh-free technique to analyze the free-surface seepage problem as a
70 moving-boundary problem has been exercised by Zhang et al. [9]. The node locations were arbitrary
71 in this meshless method letting the seepage problems with free surface be appropriately analyzed.

72 Although analytical techniques cannot straightly apply to complicated geometries and complex
73 boundary conditions, these methods, however, can provide exact solutions to problems [1].

74 Preparing approximate analysis satisfying high accuracy to deal with the more complex issues is
75 conducted by numerical methods. The approaches considered to be mesh-based, such as finite
76 difference, finite volume, and finite element, are implemented to discretize the whole problem
77 domains. An essential disadvantage of most mesh-based methods is that a domain could be
78 encountered, in cases, consisting of singular points and sharp corners, making the further progress
79 of numerical-based techniques towards the desired solution(s) numerically impossible [9-11].

80 A newly developed semi-analytical method called Scaled Boundary Finite Element Method
81 (SBFEM), proven to be capable of solving different types of differential equations, was proposed by
82 Song and Wolf [12] to transcend the limits of some existing recent approaches. The SBFEM has
83 merged important excellences of finite element and boundary element methods. Bazyar and Graili
84 [13] analyzed the confined seepage problems beneath the dams and the sheet piles in steady-state
85 conditions in anisotropic media using SBFEM. What was conducted in another part of Bazyar and
86 Graili [13] study was a successful attempt to solve unconfined flow problems using an unknown free
87 surface through the dam body. The SBFEM for analyzing the transient seepage problems in bounded
88 and unconfined domains was extended by Bazyar and Talebi [14]. The proposed method was capable
89 of solving the seepage problem for heterogeneous and anisotropic porous media without extra
90 endeavor. Reliability analysis of seepage in several numerical problems through stochastic SBFEM
91 was handled by Johari and Heydari [15]. Su et al. [16] utilized drainage substructure and nodal virtual
92 flux method to simulate drainage holes and analyze complex seepage fields. The advantages of the
93 SBFEM outweigh other methods. Hence, it seems to be a practical method to analyze the seepage
94 beneath sheet piles and to acquire the discharge flow rate.

95 Despite the efficiencies of the SBFEM in obtaining the discharge flow rate, a separate analysis
96 will be needed for discharge flow rate computing in every single condition. Furthermore, the user
97 must be fully acquainted with the analysis procedure in order to be able to effectively and efficiently
98 analyze the seepage problem beneath the sheet piles and subsequently acquire the discharge flow

99 rate. To overcome this downside, prediction models have been developed that directly relate
100 quantities such as discharge flow rate to their contributing parameters which removed the need for
101 tedious use of any analytical, numerical, or laboratory methods to calculate the discharge flow rate
102 as part of solution procedures. Data-driven approaches, regression methods, artificial intelligence,
103 and other soft computing techniques have been recently attracted several researchers to generate
104 prediction equations for the complicated behavior of various systems. Artificial Neural Networks
105 (ANN) [17, 18], Adaptive Neuro-Fuzzy Inference System (ANFIS) [19, 20], Ant Colony Optimization
106 (ACO) [21], Evolutionary Polynomial Regression (EPR) [22], Genetic Algorithm (GA) [23-25], Genetic
107 Programming (GP) [26-28], Genetic-Based Neural Network (GBNN) [29, 30], and Gene Expression
108 Programming (GEP) [31-34] can be mentioned as the most conventional soft computing and
109 heretofore outstanding contributions in various civil engineering problems.

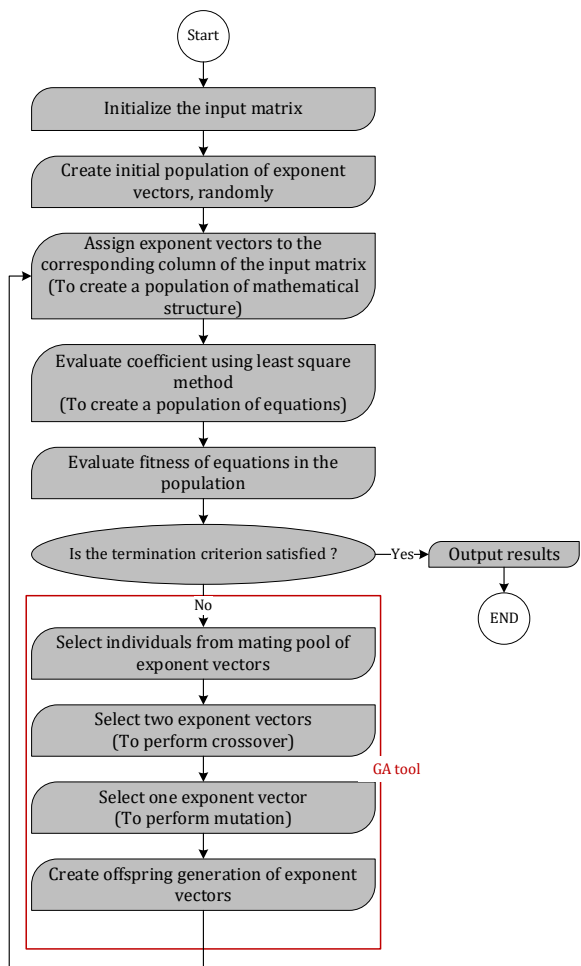
110 In this contribution, an Evolutionary Polynomial Regression (EPR) model is developed to
111 predict discharge flow rate under sheet piles. The EPR models developed in this study were produced
112 based on a large database comprising 1000 lines of artificial data retrieved from using the SBFEM
113 method simulating real-world conditions of seepage under sheet piles to provide a powerful,
114 representative, and comprehensive model that could be applied to the situations similar to the
115 conditions underlain in the comprehensive model development database used.

116 **2. Evolutionary polynomial regression (EPR)**

117 Evolutionary Polynomial Regression (EPR) is a data-driven method based on evolutionary
118 computing to search polynomial structures representing a system. A general EPR expression may be
119 presented as:

$$y = \sum_{j=1}^n F(X, f(X), a_j) + a_0 \quad (1)$$

120 where \mathbf{y} is the estimated vector of the output of the process; \mathbf{a}_j is model parameters; \mathbf{F} is a function
 121 constructed by the EPR process; \mathbf{X} is the matrix of input variables; \mathbf{f} is a function defined by the user,
 122 and \mathbf{n} is the number of terms of the target expression. The general functional structure is constructed
 123 from elementary functions by EPR using a Genetic Algorithm (GA) strategy. The GA is employed to
 124 select the useful input vectors from \mathbf{X} to be combined. The building blocks (elements) of the structure
 125 of \mathbf{F} are defined by the user based on an understanding of the physical process. While the selection
 126 of feasible structures to be combined is made through an evolutionary process, the parameters \mathbf{a}_j are
 127 estimated by the least square method (Fig. 1).



128

129

Fig. 1. Typical flow diagram for the EPR procedure

130 In this technique, the combination of the genetic algorithm to find feasible structures and the least
131 square method to find the appropriate model parameters for those structures implies some
132 advantages. In particular, the GA allows a global exploration of the error surface relevant to
133 specifically defined objective functions. By using such objective functions some criteria can be
134 selected to be satisfied through the search process. These criteria can be set in order to (a) avoid the
135 overfitting of models, (b) push the models towards simpler structures, and (c) avoid unnecessary
136 terms representative of the noise in data. EPR avoids over-fitting by penalizing the number of inputs
137 involved in structures (model complexity); controlling the constant values whose term may describe
138 noise when the related constant is close to zero, and controlling the variance of EPR terms with
139 respect to noise variance in data which is estimated by model residuals [35]. A useful feature of EPR
140 is the high level of interactivity between the user and the methodology. The user physical insight can
141 be used to make hypotheses on the elements of the target function and on its structure (Equation
142 (1)). Selecting an appropriate objective function, assuming pre-selected elements in Equation (1)
143 based on engineering judgment and working with dimensional information enable refinement of
144 final models [22].

145 Before starting the evolutionary procedure, a number of constraints can be implemented to control
146 the structure of the models to be constructed, in terms of length of the equations, type of functions
147 used, number of terms, range of exponents, number of generations etc. It can be seen that there is
148 great potential in achieving different models for a particular problem which enables the user to gain
149 additional information. By starting to apply the EPR procedure, the evolutionary process starts from
150 a constant mean of output values. By increasing the number of evolutions, it gradually picks up the
151 different participating parameters in order to form equations representing the constitutive
152 relationships. Each model is trained using the training data and tested using the testing data [22, 35].

153

154 **3. Data preparation using SBFEM**

155 The EPR models developed in this study were produced based on an extensive database including
156 1000 lines of synthetic data retrieved from the SBFEM method simulating possible scenarios under
157 various boundary and real-world conditions of seepage under sheet piles using a robust,
158 representative, and comprehensive model. Fig. 2 shows the geometry and the boundary conditions
159 of the problem domain divided into non-uniform subdomains. The sheet pile is considered in the
160 middle of the modeling domain. A 20.0m by 40.0m horizontal saturated soil layer is modeled as the
161 domain of the problem.

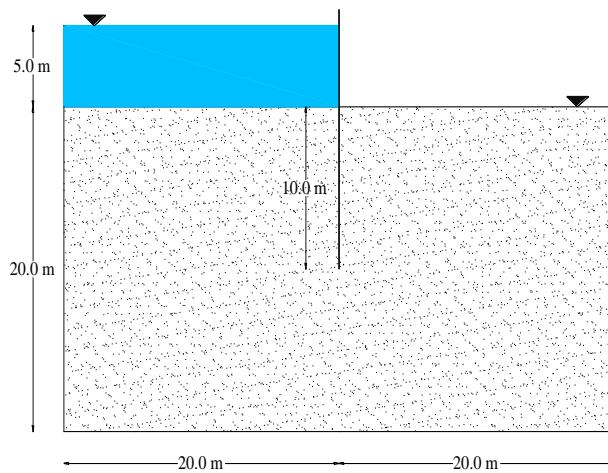
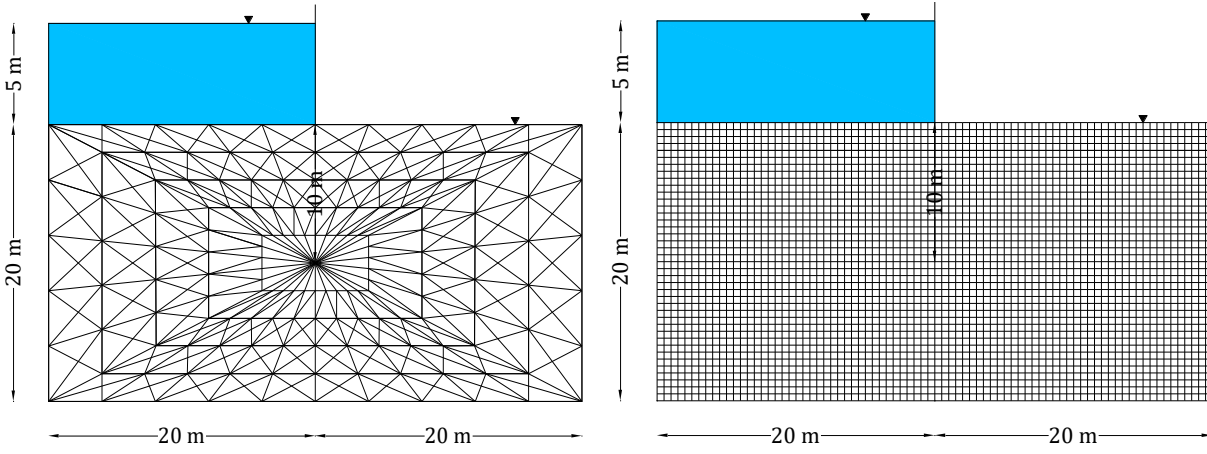


Fig. 2. The geometry of the model

162 The preciseness and versatility of the model used to produce the data based on which this research
163 was conducted are clarified by comparing the results of SBFEM with those of FEM. For this purpose,
164 an FEM code was developed. The domain discretization used for both models is shown in Fig. 3. The
165 domain is discretized into 450 subdomains for SBFEM. The scaling centers related to corresponding
166 subdomains, are located exactly at the geometry center. The contour of potential lines for the results
167 of SBFEM and FEM is demonstrated in Fig. 4. The results indicated great compatibility between the
168 results of SBFEM and FEM, a strong testimony for the accuracy and the reliability of the generated
169 artificial data used in this study.



170

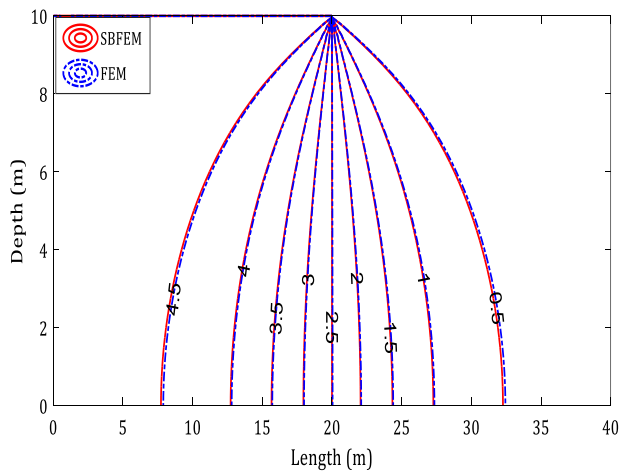
171

172

(a)

(b)

Fig. 3. Domain discretization of (a) SBFEM, (b) FEM



173

174

Fig. 4. The contour of potential lines

175 **4. Developing the EPR model**

176 In pattern recognition procedures in general, for instance neural network, fuzzy logic, or genetic
 177 programming, the model construction is normally based on adaptive learning over several cases. The
 178 performance of the developed model is then evaluated using a validation data set which has not been
 179 used/participated in the model development process. In evolutionary-based modeling, how the data
 180 are divided into training and validation sets has a significant effect on the results [36, 37].

181 The developed model could be applied to situations similar to the conditions underlain in the
 182 comprehensive model development database. Three input parameters with biggest influence on the
 183 seepage results are selected, including sheet pile height (D), upstream water level (H), and hydraulic
 184 conductivity anisotropy ratio of deposit materials (K). The output parameter is considered as the
 185 normalized flow rate Q_{Nor} . The seepage problem is an elastic problem and based on seepage equations
 186 the only soil parameter that is involved in solving the problem is the infiltration coefficient. From the
 187 geometrical point of view, upstream water level (H) and Sheet pile height (D) are the most influencing
 188 parameters, and the modelling dimensions will have little effect on the results. Results from previous
 189 studies [40] emphasize that the sheet pile height has greater effect on the total seepage discharge
 190 compared to any other location-related parameter that may affect seepage. The parameter ranges in
 191 this study are considered to fall within the expected range for small to medium sheet piles [41] that
 192 are most used in the industry. However, the EPR model has the capability to be retrained if different
 193 ranges of parameters were the subject of interest or in case any complementary data becomes
 194 available to make sure the model stays relevant and applicable to the considered newly emerging
 195 scenarios. Table 1 states the range of parameters for the input and output parameters in this
 196 research.

197 Table 1. Parameters involved in the developed EPR model

198	Parameters	Range
199	Input parameters	
200	Sheet pile's height (D)	0.25-10 m
201	Upstream water level (H)	1-5 m
202	Anisotropy ratio of deposit materials (K)	0.2-1
203	Output parameter	
	Normalized flow rate Q_{Nor}	$1.42 \times 10^{-6} - 8.54 \times 10^{-5}$

204 The training of the EPR resulted in the development of few equations. Of these, some equations did
205 not include the effect of all contributing parameters. Among the remaining equations, the most
206 appropriate and efficient one based on the model performance (fitness) and complexity was selected
207 as the final model. Equations 2 presents the developed EPR model.

$$Q_{nor} = -1.24D^3H + 2.47D^2H - 1.64DH - 0.17DK + 0.23HK + .44H + 0.14K + 0.02 \quad (2)$$

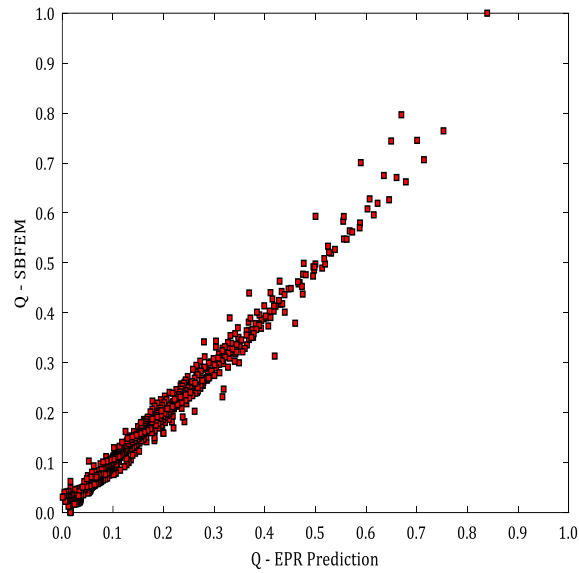
208 The D, H, and K are the cut-off depth, the upstream/upper head of water, and the anisotropy ratio
209 (k_x/k_y) of a soil deposit respectively. Fig.5 shows the normalized flow rate predicted by EPR against
210 the data used to develop the EPR model (training data).

211

212 In this study, the dataset was split into several random combinations of training and validation sets
213 until a robust representation of the whole population was achieved for both training and validation
214 sets. Statistical analysis was performed on the input and output parameters of the randomly selected
215 training and validation sets to choose the most robust representation. This was to ensure that the
216 statistical properties of the selected data in each of the subsets (training or testing) are as close as
217 possible to the other, and the training and testing subsets represent the same statistical population.
218 Of the 1000 available data sets, 80% were used to train EPR. The remaining 200 (20%) was chosen
219 to validate the developed model, meaning that these sets were unseen to EPR during the model
220 development processes. The ratio on which the data is divided into training and testing subsets is
221 chosen to stay consistent and comparable with the traditional approach in machine learning research
222 [22, 36]; however, there is no limitation in EPR approach in choosing any ratio and depending on the
223 data availability and application this could change. Many possibilities emerged, enabling the desired
224 combination of the training and testing data. Therefore, minimum, maximum, mean, and standard
225 deviation were calculated for all the contributing parameters for the training and testing datasets for
226 possible cases. The one point in which the standard deviation and mean values were the closest for

227 the training and testing data was chosen for training and testing stages in the EPR model
228 development process. In this way, the most statistically consistent combination was used to construct
229 and validate the EPR model.

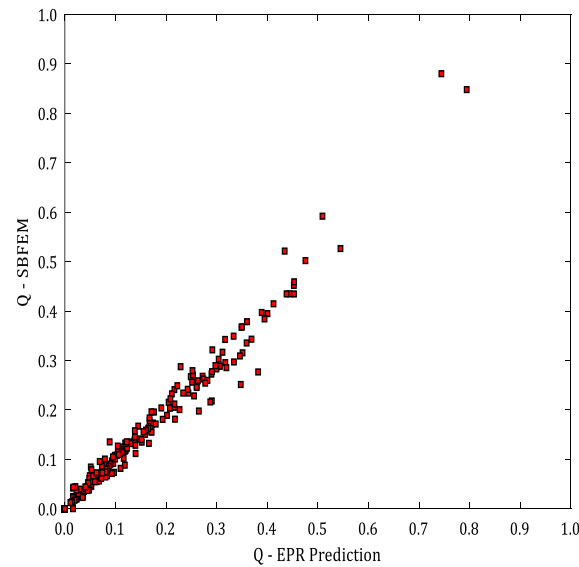
230



231

232

Fig. 5: Predicted vs. SBFEM-based data used to train EPR model



233

234

Fig. 6: Predicted vs. SBFEM-based data used to validate EPR model

235 The level of accuracy at each stage of the modelling process was evaluated based on the coefficient
236 of determination (COD) i.e., the fitness function defined as [22, 35]:

237

$$\text{COD} = 1 - \frac{\sum_N (\mathbf{Y}_a - \mathbf{Y}_p)^2}{\sum_N \left(\mathbf{Y}_a - \frac{1}{N} \sum_N \mathbf{Y}_a \right)^2} \quad (3)$$

238

239 where \mathbf{Y}_a is the actual output value; \mathbf{Y}_p is the EPR predicted value and N is the number of data
240 points on which the COD is computed. If the model fitness is not acceptable or the other termination
241 criteria (in terms of maximum number of generations and maximum number of terms) are not
242 satisfied, the current model should go through another evolution in order to obtain a new model.

243 As seen in Fig. 6, comparison of the results along with the high Coefficient of Determination (COD)
244 values for the EPR model (Training COD: 98% - Testing COD: 97%) indicate the excellent
245 performance of the developed model in capturing the underlying relationships between the
246 contributing parameters and flow rate and also in generalizing the training to predict seepage
247 behavior under sheet piles under unseen conditions.

248 The proposed EPR model generates a transparent and structured representation of the system.
249 One of the main advantages of the EPR approach is that there is no need to assume a priori form of
250 the relationship between the input and output parameters. The explicit and transparent structures
251 obtained from the proposed EPR method can allow physical interpretation of the model predictions
252 giving the user additional insight into the relationship between input and output parameters by
253 performing sensitivity analyses of the developed model for individual contributing parameters. In
254 general, EPR-based modeling has several advantages, including that it provides a simple and

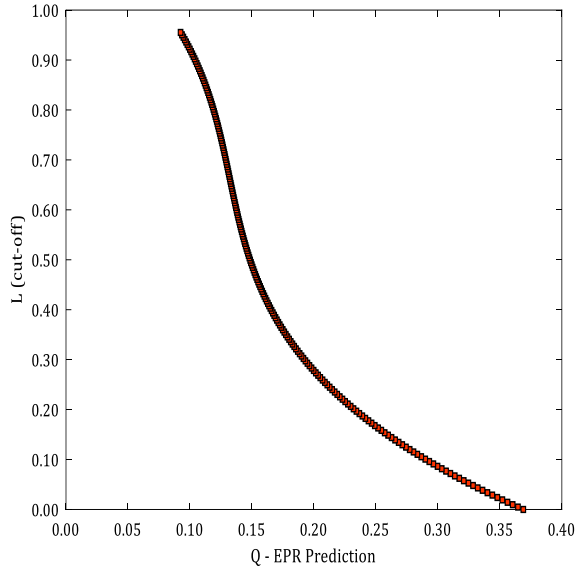
255 straightforward framework for modeling all materials. It does not require any arbitrary choice of the
256 constitutive (mathematical) model, yield function, plastic potential function, flow rule, etc. As EPR
257 learns the material behavior directly from raw experimental data, it is the shortest route from
258 experimental / research-based / artificially generated data to numerical modeling.

259 It should be noted that EPR trains and develops validated models using the data provided regardless
260 of the way the data has been collected/generated. This study is also not an exception and the
261 synthetic data generated along with its geometrical as well as any other aspects, which are
262 intrinsically included in the data, is used by EPR and the presented model reflects the data – as a
263 whole - used to train EPR and develop and validate the model, precisely as expected by the user, in
264 the model outcomes / predictions. However, EPR has the capability to be retrained where
265 more/different data is developed, needed, or becomes available to ensure the model stays
266 representative, relevant, and comprehensive.

267 **4.1. Sensitivity analysis**

268 A sensitivity analysis was conducted to investigate the effects of individual contributing
269 parameters on the predictions made by the proposed model. The aim was to verify the consistency
270 of the behavior predicted by the model and the expected behavior for the system from the literature.
271 To perform the analysis for every normalized contributing parameter, all the parameter values for
272 all parameters - other than the one being investigated - were set to their average values in the range.
273 The parameter being studied then was set to vary between the minimum and maximum parameter
274 values. A graph was then plotted to show the variations in EPR predictions for the flow rate as the
275 parameter in question varied in value between its minimum and maximum values. Figs. 7, 8, and 9
276 show the sensitivity analysis results for sheet pile/cut-off wall length, upstream/upper head, and
277 anisotropy ratio.

278



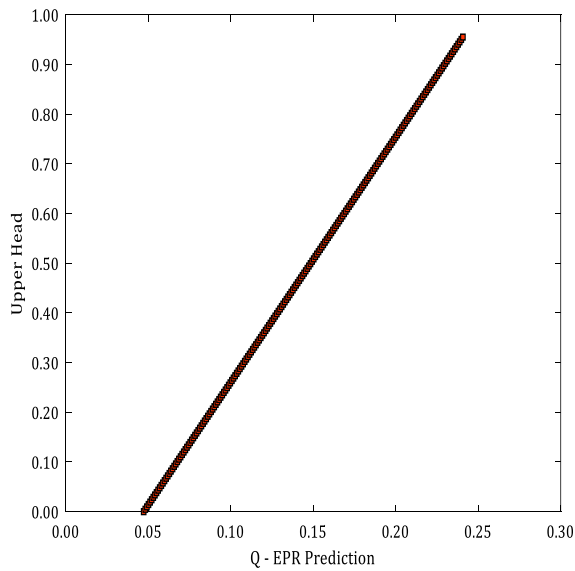
279

280

Fig. 7: Sensitivity analysis – Effect of changes in sheet pile/cut-off wall length on flow rate

281

predictions by the EPR model



282

283

Fig. 8: Sensitivity analysis – Effect of changes in upstream/upper head of water on flow rate

284

predictions by the EPR model

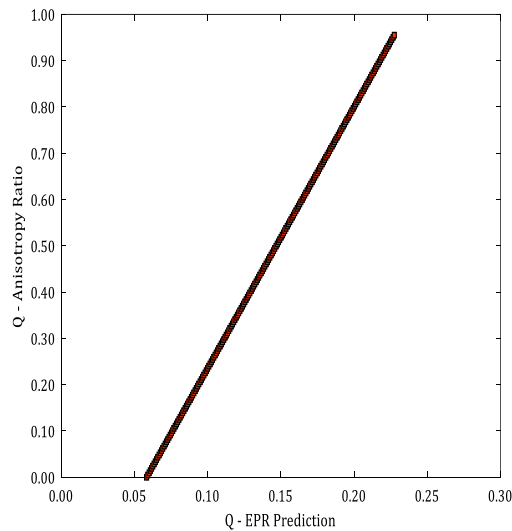
285

As seen in Fig. 7, given a certain position of the cut-off wall, increasing the cut-off depth results

286

in a reduction in the seepage discharge, and the flow rate predicted by the EPR model decreases. This

287 phenomenon can be understood based on Darcy's theory [38]. Moreover, as the opening between the
288 cut-off wall and the impervious floor is reduced, converging flow lines add resistance to the flow, and
289 seepage is diminished. As seen in Fig. 8, given a specific position of the cut-off wall, increasing the
290 upstream/upper head of water results in an increase in the seepage discharge, so the flow rate
291 predicted by the EPR model increases. If the head (h) is everywhere, there is no water flow through
292 the soil. If the head differs in different parts of the soil mass, water flows away from points at which
293 the head is high and towards points at which the head is lower. The flow rate is governed by the
294 hydraulic gradient dependent directly on the water head, which is considered the essential term of
295 the seepage force per soil volume and acts in the flow direction. When the flow is upward in the soil,
296 pore water pressure increases, and effective stress decreases. When the flow is downward, the pore
297 water pressure drops, and the effective stress increases.



298
299 Fig. 9: Sensitivity analysis – Effect of changes in anisotropy ratio on flow rate predictions by
300 the EPR model

301 As seen in Fig. 9, given a specific position of the cut-off wall, increasing the anisotropy ratio of
302 a soil deposit results in an increase in the seepage discharge, so the flow rate predicted by the EPR

303 model increases. It was found that increasing the anisotropy ratio of permeability leads to the
304 formation of horizontal flow canals and increasing the seepage flow consequently at a constant
305 vertical permeability. Variation of permeability coefficient was found to have almost no impact on
306 mean discharge flow rate for anisotropic fields compared to the isotropic conditions. Hence, it
307 appears that the anisotropic properties of the soil alluvium have a significant influence on the stress
308 distribution, hydraulic conductivity coefficient, and damage zone [39].

309 **5. Discussion and Conclusion**

310 The current study investigated an EPR model which is developed to predict discharge flow rate
311 under sheet piles. The EPR models developed in this contribution were produced based on an
312 extensive database comprising 1000 lines of artificial data retrieved from using the SBFEM method
313 simulating real-world seepage conditions under sheet piles. As mentioned before, one of the
314 important advantages of this method is modeling the singular points directly with high accuracy, and
315 this feature can be utilized to model seepage beneath the sheet piles as a singular point. The
316 preciseness and versatility of the model were clarified by comparing the results of SBFEM with those
317 of FEM. The domain was discretized into 450 subdomains and 3200 elements for SBFEM and FEM,
318 respectively. The contour of potential lines for the results of SBFEM and FEM was shown. The results
319 indicated great compatibility between the results of SBFEM and FEM.

320 A robust, representative, and comprehensive model that could be applied to situations similar
321 to the conditions underlain in the complete model development database, was developed. It was
322 shown that the EPR model can capture the underlying relationships between various parameters
323 directly from artificially developed SBFEM data and make predictions of very high precision for
324 unseen scenarios (as verified by the introduced unseen testing/verification data set). The EPR model
325 was tested using data that were not used in the training stage of the EPR model development process;
326 thus, an unbiased performance indicator was obtained on the actual prediction capability of the

327 model. The results show the excellent ability of the EPR model in generalizing the training to predict
328 flow rates under unseen conditions. Ultimately, the validity of the behavior consistency, signified by
329 the model and the expected system behavior from the literature, has been assessed by sensitivity
330 analysis. Accordingly, the Q_{nor} predicted by the EPR model decreases when the cut-off depth increases
331 at a particular position of the cut-off wall. The training of the EPR resulted in the development of few
332 equations. Since some equations did not include all contributing parameters, the most appropriate
333 and efficient one based on the model performance (fitness) and complexity was selected as the final
334 model. After training the desired EPR model, its account was verified using 200 sets of validation data
335 that had not been introduced to EPR during training. Then a comparison between COD values for the
336 EPR models, including training and testing CODs (i.e., training COD: 98% - testing COD: 97%), has
337 been drawn to prove the appropriate fitness of the developed model in capturing the underlying
338 relationships between the contributing parameters and flow rate and also in generalizing the training
339 to predict seepage behavior under sheet piles under unseen conditions. This obtained parameter has
340 also increased when the upstream/upper head of water and the soil deposit's anisotropy ratio
341 increased.

342 The synthetic data used to develop and verify the EPR model has been carefully generated to
343 be robust and to represent real world problems. The developed model verification and parametric
344 study suggest that the model predictions are in line with expectations and are highly accurate as long
345 as the contributing parameters of any problem fall in the ranges used to create and verify the model;
346 however, it is advised that necessary precautions and verifications to be put in place on case-by-case
347 basis and where applying the model to real world problems to ensure safety of the structures.

348 **References**

- 349 [1] J.-H. He, "Approximate analytical solution for seepage flow with fractional derivatives in
350 porous media," *Computer Methods in Applied Mechanics and Engineering*, vol. 167, no. 1-2, pp.
351 57-68, 1998.
- 352 [2] Y. Jie, G. Jie, Z. Mao, and G. Li, "Seepage analysis based on boundary-fitted coordinate
353 transformation method," *Computers and Geotechnics*, vol. 31, no. 4, pp. 279-283, 2004.
- 354 [3] T. Fukuchi, "Numerical analyses of steady-state seepage problems using the interpolation
355 finite difference method," *Soils and Foundations*, vol. 56, no. 4, pp. 608-626, 2016.
- 356 [4] E. Bresciani, P. Davy, and J.-R. de Dreuzy, "A finite volume approach with local adaptation
357 scheme for the simulation of free surface flow in porous media," *International Journal for*
358 *Numerical and Analytical Methods in Geomechanics*, vol. 36, no. 13, pp. 1574-1591, 2012.
- 359 [5] A. Ouria, M. M. Toufigh, and A. Nakhai, "An investigation on the effect of the coupled and
360 uncoupled formulation on transient seepage by the finite element method," *Am J Appl Sci*, vol.
361 4, no. 12, pp. 950-956, 2007.
- 362 [6] M. J. Kazemzadeh-Parsi and F. Daneshmand, "Three dimensional smoothed fixed grid finite
363 element method for the solution of unconfined seepage problems," *Finite Elements in Analysis*
364 *and Design*, vol. 64, pp. 24-35, 2013.
- 365 [7] K. Rafiezadeh and B. Ataie-Ashtiani, "Transient free-surface seepage in three-dimensional
366 general anisotropic media by BEM," *Engineering Analysis with Boundary Elements*, vol. 46, pp.
367 51-66, 2014.
- 368 [8] Y.-x. Jie, L.-z. Liu, W.-j. Xu, and G.-x. Li, "Application of NEM in seepage analysis with a free
369 surface," *Mathematics and computers in simulation*, vol. 89, pp. 23-37, 2013.

- 370 [9] W. Zhang, B. Dai, Z. Liu, and C. Zhou, "Unconfined seepage analysis using moving kriging
371 mesh-free method with Monte Carlo integration," *Transport in Porous Media*, vol. 116, no. 1,
372 pp. 163-180, 2017.
- 373 [10] F. Motaman, G. Rakhshandehroo, M. Hashemi, and M. Niazkar, "Application of RBF-DQ
374 method to time-dependent analysis of unsaturated seepage," *Transport in Porous Media*, vol.
375 125, no. 3, pp. 543-564, 2018.
- 376 [11] X. Lei, S. He, X. Chen, H. Wong, L. Wu, and E. Liu, "A generalized interpolation material point
377 method for modelling coupled seepage-erosion-deformation process within unsaturated
378 soils," *Advances in Water Resources*, vol. 141, p. 103578, 2020.
- 379 [12] C. Song and J. P. Wolf, "The scaled boundary finite-element method—alias consistent
380 infinitesimal finite-element cell method—for elastodynamics," *Computer Methods in applied
381 mechanics and engineering*, vol. 147, no. 3-4, pp. 329-355, 1997.
- 382 [13] M. H. Baziyar and A. Graili, "A practical and efficient numerical scheme for the analysis of
383 steady state unconfined seepage flows," *International Journal for Numerical and Analytical
384 Methods in Geomechanics*, vol. 36, no. 16, pp. 1793-1812, 2012.
- 385 [14] M. H. Baziyar and A. Talebi, "Transient seepage analysis in zoned anisotropic soils based on
386 the scaled boundary finite-element method," *International Journal for Numerical and
387 Analytical Methods in Geomechanics*, vol. 39, no. 1, pp. 1-22, 2015.
- 388 [15] A. Johari and A. Heydari, "Reliability analysis of seepage using an applicable procedure based
389 on stochastic scaled boundary finite element method," *Engineering Analysis with Boundary
390 Elements*, vol. 94, pp. 44-59, 2018.

- 391 [16] H. Su, J. Li, Z. Wen, Z. Guo, and R. Zhou, "Integrated certainty and uncertainty evaluation
392 approach for seepage control effectiveness of a gravity dam," *Applied Mathematical*
393 *Modelling*, vol. 65, pp. 1-22, 2019.
- 394 [17] J.-X. Xie, C.-T. Cheng, K.-W. Chau, and Y.-Z. Pei, "A hybrid adaptive time-delay neural network
395 model for multi-step-ahead prediction of sunspot activity," *International journal of*
396 *environment and pollution*, vol. 28, no. 3-4, pp. 364-381, 2006.
- 397 [18] R. Taormina, K.-w. Chau, and R. Sethi, "Artificial neural network simulation of hourly
398 groundwater levels in a coastal aquifer system of the Venice lagoon," *Engineering Applications*
399 *of Artificial Intelligence*, vol. 25, no. 8, pp. 1670-1676, 2012.
- 400 [19] H. M. Azamathulla, C. K. Chang, A. A. Ghani, J. Ariffin, N. A. Zakaria, and Z. A. Hasan, "An ANFIS-
401 based approach for predicting the bed load for moderately sized rivers," *Journal of Hydro-*
402 *Environment Research*, vol. 3, no. 1, pp. 35-44, 2009.
- 403 [20] H. M. Azamathulla and A. A. Ghani, "ANFIS-based approach for predicting the scour depth at
404 culvert outlets," *Journal of pipeline systems engineering and practice*, vol. 2, no. 1, pp. 35-40,
405 2011.
- 406 [21] W. Gao, "Premium-penalty ant colony optimization and its application in slope stability
407 analysis," *Applied Soft Computing*, vol. 43, pp. 480-488, 2016.
- 408 [22] A. Ahangar-Asr, A. A. Javadi, A. Johari, and Y. Chen, "Lateral load bearing capacity modelling
409 of piles in cohesive soils in undrained conditions: an intelligent evolutionary approach,"
410 *Applied Soft Computing*, vol. 24, pp. 822-828, 2014.
- 411 [23] C.-T. Cheng, W.-C. Wang, D.-M. Xu, and K. W. Chau, "Optimizing hydropower reservoir
412 operation using hybrid genetic algorithm and chaos," *Water Resources Management*, vol. 22,
413 no. 7, pp. 895-909, 2008.

- 414 [24] A. Johari, A. Javadi, and G. Habibagahi, "Modelling the mechanical behaviour of unsaturated
415 soils using a genetic algorithm-based neural network," *Computers and Geotechnics*, vol. 38,
416 no. 1, pp. 2-13, 2011.
- 417 [25] Y. Yalcin, M. Orhon, and O. Pekcan, "An automated approach for the design of Mechanically
418 Stabilized Earth Walls incorporating metaheuristic optimization algorithms," *Applied Soft
419 Computing*, vol. 74, pp. 547-566, 2019.
- 420 [26] H. Vardhan, A. Garg, J. Li, and A. Garg, "Measurement of stress dependent permeability of
421 unsaturated clay," *Measurement*, vol. 91, pp. 371-376, 2016.
- 422 [27] W.-H. Zhou, A. Garg, and A. Garg, "Study of the volumetric water content based on density,
423 suction and initial water content," *Measurement*, vol. 94, pp. 531-537, 2016.
- 424 [28] A. Mishra, B. Kumar, and S. Vadlamudi, "Prediction of hydraulic conductivity for soil-
425 bentonite mixture," *International Journal of Environmental Science and Technology*, vol. 14,
426 no. 8, pp. 1625-1634, 2017.
- 427 [29] A. Johari, G. Habibagahi, and A. Ghahramani, "Prediction of SWCC using artificial intelligent
428 systems: A comparative study," *Scientia Iranica*, vol. 18, no. 5, pp. 1002-1008, 2011.
- 429 [30] A. Johari, G. Habibagahi, and A. Ghahramani, "Prediction of a Soil-Water Characteristic Curve
430 Using a Genetic-Based Neural Network," *Scientia Iranica*, vol. 13, no. 3, pp. 284-294.
- 431 [31] H. M. Azamathulla, "Gene-expression programming to predict friction factor for Southern
432 Italian rivers," *Neural Computing and Applications*, vol. 23, no. 5, pp. 1421-1426, 2013.
- 433 [32] A. Guven and H. M. Azamathulla, "Gene-expression programming for flip-bucket spillway
434 scour," *Water Science and technology*, vol. 65, no. 11, pp. 1982-1987, 2012.
- 435 [33] H. M. Azamathulla, "Gene expression programming for prediction of scour depth downstream
436 of sills," *Journal of Hydrology*, vol. 460, pp. 156-159, 2012.

- 437 [34] A. Johari and H. Golkarfard, "Reliability analysis of unsaturated soil sites based on
438 fundamental period throughout Shiraz, Iran," *Soil Dynamics and Earthquake Engineering*, vol.
439 115, pp. 183-197, 2018.
- 440 [35] O. Giustolisi and D. A. Savic, "A symbolic data-driven technique based on evolutionary
441 polynomial regression," *Journal of Hydroinformatics*, vol. 8, no. 3, pp. 207-222, 2006.
- 442 [36] A. A. Javadi, M. Rezaia, and M. M. Nezhad, "Evaluation of liquefaction induced lateral
443 displacements using genetic programming," *Computers and Geotechnics*, vol. 33, no. 4-5, pp.
444 222-233, 2006.
- 445 [37] M. Rezaia and A. A. Javadi, "A new genetic programming model for predicting settlement of
446 shallow foundations," *Canadian Geotechnical Journal*, vol. 44, no. 12, pp. 1462-1473, 2007.
- 447 [38] M. E. Harr, "Groundwater and seepage," *Soil Science*, vol. 95, no. 4, p. 289, 1963.
- 448 [39] T. Yang, P. Jia, W. Shi, P. Wang, H. Liu, and Q. Yu, "Seepage–stress coupled analysis on
449 anisotropic characteristics of the fractured rock mass around roadway," *Tunnelling and
450 underground space technology*, vol. 43, pp. 11-19, 2014.
- 451 [40] D. A. El Molla, " Seepage through homogeneous earth dams provided with a vertical
452 sheet pile and formed on impervious foundation," *Ain Shams Engineering Journal*, vol. 10, pp. 529-539,
453 2019.
- 454 [41] G. Gazetas, E. Garini, and A. Zafeirakos, " Seismic analysis of tall anchored sheet-pile walls," *Soil
455 Dynamics and Earthquake Engineering*, vol. 91, pp. 209-221, 2016.

456

457 **Conflict Of Interest statement**

458 There is no conflict of interest (financial or non-financial) that authors are aware of.

